

Article

Comparative Analysis of Coastal Flooding Vulnerability and Hazard Assessment at National Scale

Marcello Di Risio ^{1,*},, Antonello Bruschi ^{2,†}, Iolanda Lisi ^{2,†}, Valeria Pesarino ^{2,†} and Davide Pasquali ^{1,†}

¹ Department of Civil, Construction-Architectural and Environmental Engineering Department (DICEAA)—Environmental and Maritime Hydraulic Laboratory (LIAM), University of L'Aquila, L'Aquila 67100, Italy; davide.pasquali@univaq.it

² Italian National Institute for Environmental Protection and Research (ISPRA), Rome 00144, Italy; antonello.bruschi@isprambiente.it (A.B.); iolanda.lisi@isprambiente.it (I.L.); valeria.pesarino@isprambiente.it (V.P.)

* Correspondence: marcello.dirisio@univaq.it; Tel.: +39-(0)862-4345-34

† These authors contributed equally to this work.

Received: 8 August 2017; Accepted: 27 October 2017; Published: 2 November 2017

Abstract: The evaluation of the coastal hazard and vulnerability caused by storm conditions is an important issue related to coastal flooding and erosion. Although these topics have been widely tackled by past research, they cannot be avoided, but need to be carefully managed by local authorities in order to limit damage to coastal infrastructure, to protect human life, habitats and sensitive species. Usually, this issue is tackled through common approaches at the regional scale. This paper illustrates the first steps of a research project aimed at assessing coastal hazard and vulnerability to wave-induced flooding at the national scale. In order to apply the method to the national scale, it is necessary to select a suitable dataset. This has to be consistent with the whole application area, concerning its spatial distribution, reliability and availability. Thus, one of the aims of this project is to perform a comparative analysis using data available at the national and local scale. The analysis was performed for the area of Montalto di Castro (Tyrrhenian Sea) by using datasets with different spatial resolutions. The results revealed that the use of low resolution data does not significantly affect the estimated nearshore wave features, while the wave runup is underestimated by about 25%. This underestimation influences also the vulnerability and hazard assessments. In particular, the vulnerability is conservatively assessed if low resolution data are used. On the other hand, the hazard is conservatively assessed when low resolution data are used only if the wave runup is amplified by considering the 25% underestimation. The results presented herein can be extended to other sites with the same general features (i.e., microtidal and dissipative coastal stretches).

Keywords: coastal vulnerability; coastal hazard; coastal flooding; risk and probability

1. Introduction

This paper deals with flooding related to storm events. This is a threat to life and to socioeconomic and environmental assets. Moreover, the erosion phenomena intimately related to flooding events may worsen the threat. Coastal managers and policy makers need to make effective and timely decisions on the use of resources in the immediate and longer term (e.g., [1–5]). Thus, for a proper assessment

and management of the coastal risk, the interactions of the main physical variables (i.e., coastal geomorphology, coastal slope, shoreline evolution, mean spring tide range, wave climate) must be analyzed at different spatial and time scales. Therefore, there is the need to integrate tools able to take into account, at different complexity levels, the interactions between the main factors that drive coastal hydrodynamic and sediment transport patterns (e.g., [6–8]).

Coastal risk is the result of the interaction of one (or more) hazards and one (or more) stakes (i.e., human, economic or environmental value of the elements exposed to the hazard); while, coastal vulnerability is considered as “the capacity of a system to sustain hazardous events based on its fragility, taking into account both the hazard and the structural factors (the socioeconomic, cultural, political, and institutional context)” [1]. Thus, coastal risk is related to a future situation that has a more-or-less high probability of occurrence, then it is clearly different from dangerous events’ management. However, it has been observed that different interpretations of the same concepts (i.e., the vulnerability, the hazard and the related risk) may lead to different studies and conclusions (e.g., [9,10]). FLOODsite (e.g., [11]) defines the flood risk as two alternatives. The first one ($\text{risk} = \text{hazard} \times \text{exposure} \times \text{vulnerability}$) makes use of three elements: floods posing a hazard, i.e., a phenomenon that potentially has destructive effects; exposure, i.e., the (value of) elements exposed to hazard and vulnerability (of the area of interest, as well as of the society) that can be destructed by hazard. The second definition ($\text{risk} = \text{probability} \times \text{consequences}$) takes into account the probability of the flood. Herein, the coastal “vulnerability” is used to classify the coastal stretch features (i.e., geomorphology, coastal slope, mean significant wave height) according to a degree scale (from low to very high vulnerability, [10]). On the other hand, the coastal “hazard” is defined as the probability of occurrence of a natural phenomenon that induces coastal flooding (i.e., [10]). Accordingly, a Coastal Vulnerability Index (e.g., [12]) and a Coastal Hazard Index were both evaluated in the study illustrated herein. It has to be stressed that the “exposure” needed to evaluate the coastal risk, i.e., the evaluation of elements exposed to hazards based on the analysis of the economic value of elements at risk, is not tackled at all in the present paper. To satisfy the requirements of the Floods Directive 2007/60/EC, which includes regulations to evaluate and manage flood risks both from rivers and along EU coastlines, some European States have adopted methodologies at the national scale, others at the regional scale [13,14]. In Italy, coastal vulnerability is usually evaluated by the local authority at the regional scale, where the development of methodologies able to produce risk maps for coastal flooding is now an urgent matter (e.g., [4]). This depends on the high frequency of storm events that impact Italian coasts, often characterized by the presence of relevant economic and commercial activities, of protected and/or sensitive marine-coastal habitats (sensu the Habitat Directive, e.g., [15]).

The first step for the coastal vulnerability and hazard assessment is the evaluation of the site characteristics. In order to study all the changing patterns within a coastal system, modeling approaches are often adopted to model waves, water levels and morphological features (e.g., [2,16–19]) applicable at different scales. However, the development of a replicable approach applicable at the national scale requires a suitable and homogeneous (in terms of its spatial distribution, reliability and availability) dataset on the whole area of interest and modeling approaches whose results must be reliable for different coastal expositions (i.e., morphological type).

Within the research described herein, significant wave heights were considered to evaluate wave runup along the coast, by using standard empirical formulations. Indeed, wave runup is of utmost importance to coastal engineers, land planners and environmental managers (e.g., [20]) as it plays a crucial role in beach dynamics and in defining back lines (for different storm events) for private or municipal planning/projects. However, there are some complications related to the application of available formulations on sandy beaches (e.g., [21]) because the formulas were historically derived for hard structures with steep slopes, while sandy beaches tend to have much flatter slopes and move

freely in response to wave action (e.g., [21,22]). For this reason, in the last few decades, researchers paid attention to the wave runup estimation also for irregular waves on natural beaches. The first empirical formulations rely on the hypothesis of regular waves impinging the shore (e.g., [23–26]), based on physical model tests. Afterwards, irregular wave runup was investigated in order to extend the formulation to real-world sea states and natural beaches (e.g., [27–32]).

This paper aims to illustrate the results of the first steps of a method for evaluating the coastal vulnerability and hazard at the national scale. The main goal of the whole research is to provide a general method aimed at providing a preliminary fast evaluation of the vulnerability and hazard of storm-induced flooding. Therefore, the proposed method has to use parameters related to the main morphological features (e.g., emerged and submerged beach extension, beach slope, water depth) and to the wave climate (e.g., offshore and nearshore wave climate, storm surge). Indeed, a series of field data is usually available at the national scale that allows one to estimate, even if with a lower reliability if compared to local scale data, the emerged beach features (i.e., DEM provided by national or international institutions, e.g., [33]), along with the submerged beach features (i.e., bathymetric data provided by national or international institutions, e.g., [34]) and wave climate (i.e., wave buoy networks or mareographic stations networks or meteorological centers, e.g., [35,36]). In other words, the aim of the project is to develop a uniform approach, replicable at the national scale, aimed at evaluating the preliminary assessment of coastal vulnerability and hazard related to flooding, the first steps for coastal risk assessment, thus useful as a decision support tool for coastal zone management.

In order to assess the reliability of the method, a comparative analysis was performed for the area of Montalto di Castro (Tyrrhenian Sea, Italy) as a case study. By using datasets with different spatial resolutions, the results (i.e., coastal vulnerability and hazard indexes) were compared and the reliability assessed.

The paper is structured as follows. The next section is aimed at giving the details of the employed methods. Then, the study area and available data are described in the succeeding section. Section 4 illustrates and discusses the main results of the study. Concluding remarks and the description of the ongoing research close the paper.

2. Methods

This paper aims to illustrate the first step of a methodology for coastal flooding risk assessment (Figure 1). The shaded boxes in the bottom-left part of the workflow of Figure 1 highlight the issues actually addressed in this paper. Indeed, the research aims to evaluate, at least within a preliminary stage, the role of the reliability of wave climate and beach morphology upon the coastal vulnerability and hazard assessments in order to provide a method to be applied at the national scale. Such a method demands several considerations that may have an impact on the results in terms of vulnerability and hazard assessments: the viability of the analysis at the national scale, the availability of field data, the sensibility of the results to the wave runup estimates, etc. The present papers aims to analyze the role of the resolution of the field data to the results of vulnerability and hazard assessments. Therefore, the field data have to be available and homogeneous at the national scale.

The selected sources exist in European databases as the one provided within EMODnet for bathymetry (European Marine Observation and Data Network, e.g., [34]) and by the ECMWF (European Centre for Medium Range Weather Forecast) open database ERA-Interim for sea waves [36]. Furthermore, data provided by the Italian buoy network (managed by ISPRA) and the DEM (digital elevation model) produced by the Italian Ministry for the Environment were used (hereinafter “national scale data”).

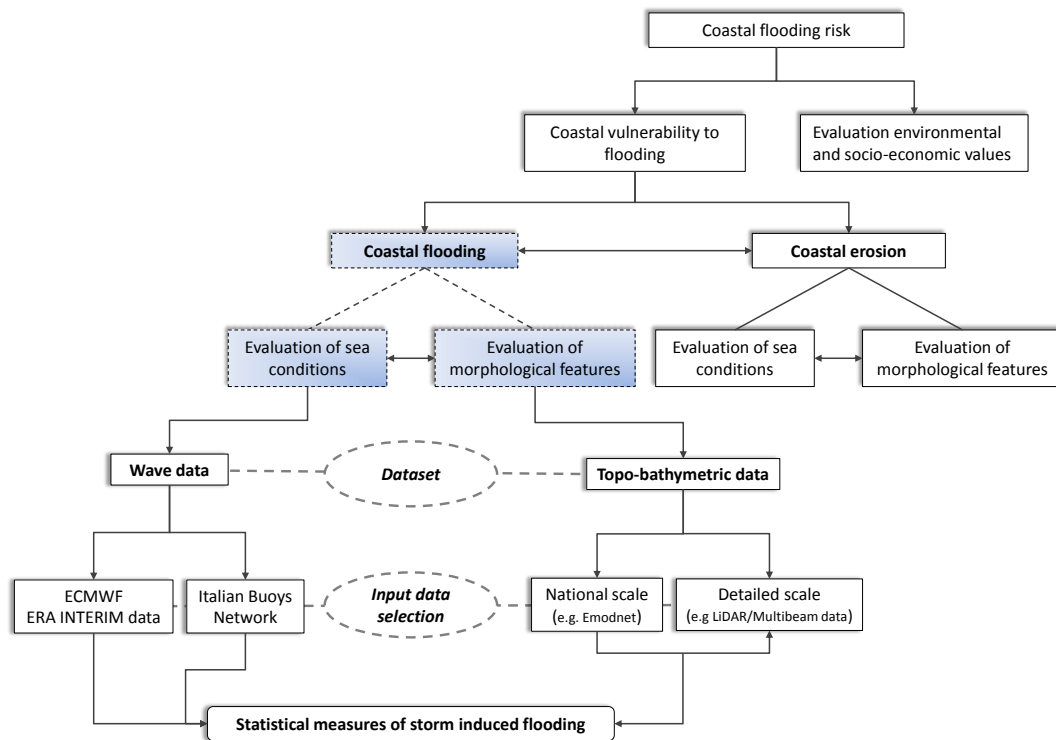


Figure 1. Workflow of risk assessment. The shaded boxes highlight the issues tackled in this work.

These data are used to set up input data and a modeling scenario to propagate sea waves toward the coast. The results have been compared with those obtained by the same scenario built on detailed data (hereinafter “local scale data”), only available at the local scale in some areas; in particular, LiDAR and multibeam data were used to model the bathymetric configuration.

Then, both national-scale and local-scale data were used, and:

- nearshore wave conditions;
- wave runoff;
- Coastal Vulnerability Index;
- Coastal Hazard Index

were estimated in order to evaluate the influence of the resolution of the data on the vulnerability and hazard assessments.

2.1. Nearshore Wave Conditions

The SWAN model (Simulating WAVes Nearshore, e.g., [37]) was used to propagate the off-shore wave conditions towards the coast up to water depths equal to 20 m, 10 m and 5 m. The offshore wave climate used to force the model at the boundary is obtained from the ECMWF ERA-Interim dataset (grid point closest to the buoy of Civitavecchia location belonging to the National Buoy Network, period 1979–2015). These data have been corrected by comparison with in situ data from the RONbuoy of Civitavecchia. This was achieved by evaluating a calibration factor to solve the known problem of the underestimation of the wave height (e.g., [38]) in the ERA-Interim database.

The data were classified in terms of significant wave height (H_{m0}) and the mean direction (D_m) joint frequency table (hereinafter $H_{m0} - D_m$ JFT). Classes used in the table are identified by 0.5 m-wide bins for the wave height and 10 deg-wide bins for the direction. Then, only one element from each class of the table was selected to be used as the boundary condition for the SWAN model. The representative element selected from each class is the central one (with respect to the significant wave height and

mean direction ranges of variation within the class). In this way, the number of sea states to be propagated towards the coast is reduced from many thousands (i.e., the whole offshore time series) to a few hundreds. The only issue to solve is the lack of a period (i.e., the peak period T_p) to be assigned to the $H_{m0} - D_m$ couples characterizing the representative elements of the table. The issue is solved by analyzing the original data through a significant wave height-peak period joint frequency table (hereinafter $H_{m0} - T_p$ JFT). Then, each $H_{m0} - D_m$ couple obtained from the $H_{m0} - D_m$ JFT is completed with the T_p corresponding to the most populated classes in the $H_{m0} - T_p$ JFT, corresponding to the H_{m0} value in the $H_{m0} - D_m$ couple. The $H_{m0} - D_m - T_p$ trios obtained in this way, representing the whole wave climate in the area, have been propagated toward the coast through the SWAN model as stationary conditions. The next step is to decompose each element in the ECMWF ERA-Interim corrected dataset in a bilinear interpolation of classes present in the $H_{m0} - D_m$ JFT. Then, the coastal propagation of each sea state is obtained using the same interpolation factors applied to the elements corresponding in the transfer function to the elements of the $H_{m0} - D_m$ JFT used in the bilinear interpolation.

2.2. Wave Runup

The seminal work carried out by Hunt [26] first addressed the influence of the Iribarren number [28] upon the wave runup on smooth slopes, related to the wave runup on coastal structures (e.g., [39]). The Iribarren number (ζ_0 , also known as the surf similarity parameter) aims to relate the slope of the beach (or coastal structure, β) to the offshore wave steepness ($= H_0/L_0$, H_0 being the offshore wave height and $L_0 = g/2/\pi T^2$ the offshore wave length evaluated on the basis of wave period T):

$$\zeta_0 = \frac{\tan \beta}{\sqrt{H_0/L_0}}. \quad (1)$$

Other definitions of the Iribarren number may be found when different wave heights (i.e., breaking wave height) or wave periods (i.e., either the peak or mean wave period) are used.

A few years later, Guza and Thornton [40] studied extensively the statistics of swash on natural beaches both in the laboratory and in the field. They found that the significant wave runup (including both wave setup and runup) is linearly proportional to the significant deep-water wave height. This was observed to be true only for low Iribarren numbers by Holman and Sallenger [41]. They analyzed a series of field data for a moderately steep beach (Duck, North Carolina), and they found a rough linear trend between the non-dimensional setup (normalized by using the offshore wave height) and the Iribarren number. Then, Holman [29] used the same data as Holman and Sallenger [41] in order to get an estimate of the 2% exceedance level of wave runup. The data were observed to be well parameterized in terms of Iribarren number. Moreover, it was observed that the total runup is more scattered than the wave runup (i.e., the total runup but the swash component). The research works performed by Mase and Iwagaki [42] and Mase [43] were among the first ones aimed at experimentally investigating the runup of irregular waves on gentle slopes made of smooth and impermeable materials. They gave a power law able to estimate some statistical measures (i.e., maximum value, mean value, 2% exceedance level) of the non-dimensional wave runup as a function of the Iribarren number. Later, Nielsen and Hanslow [30] performed a study on a wide range of natural beach (i.e., from reflective to dissipative) by observing that the influence of the Iribarren number on the wave runup is rather limited for flat beaches (i.e., for $\tan \beta_f \leq 0.10$, with β_f the beach face slope). This aspect was also highlighted by Douglass [22] who reanalyzed the data of Holman [29] by observing that the wave runup data show little dependence on the beach slope. It is worthy to notice that the field data of Holman refer to a moderately steep beach (Duck, NC, USA) for which $\tan \beta_f \simeq 0.1$, thereby confirming the results of Nielsen and Hanslow [30]. The low influence of beach

slope for flat beaches was further confirmed by Ruggiero et al. [44] for dissipative beaches (Oregon). Stockdon et al. [31] decomposed the wave runup into the wave setup, i.e., the time-average of the water level elevation at the shoreline and the swash (both in the incident and infragravity band), i.e., the time-varying fluctuation of the water level about the wave setup. By analyzing a wide dataset for beach foreshore slope β_f within the range 0.01–0.11, they proposed a general relationship giving the 2% exceedance level of wave runup (R_2):

$$R_2 = 1.1 \left\{ 0.35\beta_f\sqrt{H_0L_0} + \frac{1}{2} \left[H_0L_0 \left(0.563\beta_f^2 + 0.004 \right) \right]^{1/2} \right\}, \quad (2)$$

and by confirming that for the dissipative beach (i.e., $\xi_0 < 0.3$, with ξ_0 the Iribarren number estimated with offshore wave height and wave length), the beach slope plays a minor role:

$$R_2 = 0.043\sqrt{H_0L_0}, \quad (3)$$

It has to be stressed that beach slope β_f in Relationship (2) was defined as the average slope over a (vertical) region $\pm\sigma$, with σ equal to the standard deviation of the continuous water level record. It has been demonstrated that Equation (2) provides a reasonable estimation also under hurricane surge and wave conditions and for coastal berms and dunes by adopting the runup Iribarren number and berm reduction factor proposed by Park and Cox [45]. Further, Roberts et al. [46] analytically demonstrated that for flat sandy beaches, the total wave runup is not a function of beach slope if bottom friction is neglected, and they proposed a rather simple relationship for which the total wave runup equals the significant breaking wave height based on movable experimental large-scale tests. As the beach slope is usually hard to estimate, Mather et al. [47] proposed an empirical formulation based on the estimation of a representative beach slope up to the 15-m offshore contour, successfully applied to a case study along the South Africa coastline. Polidoro et al. [48] proposed to use spectral parameters (i.e., peakedness parameter) and the Iribarren number estimated by using the spectral mean period for a shingle beach (i.e., rather steep beaches).

It is rather clear that the wave runup has been extensively studied, and many empirical formulations are available in the literature. In the research presented herein, the wave runup elevations were estimated for the two considered scenarios, i.e., by using data available at the national scale and data available only at the local scale, by means of the empirical Formulation (2) as proposed by Stockdon et al. [31].

2.3. Coastal Vulnerability Index and Coastal Hazard Index

In order to assess the coastal vulnerability, i.e., to classify the coastal stretch in terms of its physical features related to the proneness to coastal flooding, the Coastal Vulnerability Index (CVI) proposed by Gornitz et al. [12] and used by several studies (e.g., [10,49–51]) has been considered. The CVI has been modified and used for the case study described in Section 3 in order to adapt it to the intrinsic parameters of the considered area.

In particular, factors aimed at describing the slope of the submerged beach (F_S), the extension of the area prone to be flooded (F_A), the distance away from the coastline of the -10.0 -m contour (F_D) and the nearshore mean significant wave height (F_W) are considered:

$$CVI = \sqrt{\frac{F_S F_A F_D F_W}{4}}. \quad (4)$$

Each factor can be converted to a 1–4 scale, Class 1 being aimed at indicating low vulnerability and Class 4 indicating very high vulnerability. With respect to other studies (e.g., [49,51]), the “very

low” and “low” rankings of coastal vulnerability have been merged together. It could be stressed that the results are not affected by this assumption, at least for “moderate”, “high” and “very high” vulnerability assessments. Usually, the ranking of each factor is based on qualitative reasoning and on the distribution of the data (i.e., the quartile range if four ranks are used) of the area of interest (e.g., [49]). As the present work is aimed at assessing the vulnerability of a rather small study area, the ranking of each factor has been defined on the basis of the literature review (e.g., [10,49–51]) and of typical values of Italian coasts.

The factor F_S , used to describe the slope of submerged beach, has been defined by evaluating the mean slope of the considered cross-section spanning the vertical region from the reference depth (i.e., 10 m) up to the coastline. The ranking of the factor F_S has been defined on the basis of the suggestions of Martínez-Grana et al. [51]: the higher the slope, the lower the coastal vulnerability (see Table 1).

The factor F_A , used to describe the extension of the flooded area, has been defined as the horizontal distance from the coastline up to the +2.0-m contour inland. The ranking of this factor has been defined by means of the same rationale of the definition of the ranking of factor F_S : the higher the extension of the flooded area, i.e., the lower the emerged beach slope, the higher the coastal vulnerability (see Table 1).

Table 1. Factors ranking needed to evaluate the Coastal Vulnerability Index (CVI).

Factor	Low (1)	Moderate (2)	High (3)	Very High (4)
F_S (deg)	>2.3	1.1–2.3	0.6–1.1	<0.6
F_A (m)	<50	50–105	105–190	>190
F_D (m)	<250	250–500	500–1000	>1000
F_W (m)	<2.0	2.0–3.0	3.0–4.0	>4.0

The factor F_D , used to describe the morphodynamic activity of the beach, has been defined as the horizontal distance of the reference water depth (i.e., 10 m) from the coastline. The ranking of this factor has been defined by observing that the higher the distance of the reference water depth, the higher the storm surge (i.e., [52]), the higher the vulnerability.

The factor F_W , aimed at describing the wave climate, has been defined as the mean value of the annual maximum of significant wave height at the nearshore limit (i.e., at a water depth equal to 10 m).

It has to be observed that the selection of the parameters to be considered in the analysis depends on the identification of the significant driving processes (e.g., [10]). Indeed, the number and type of parameters to be included in the definition of CVI change as the study area changes (e.g., [12,49,51]). In the analysis presented herein, some driving processes have been neglected as they are assumed as insignificant or out of the scope of the analysis, such as tidal range factor and sea level factor (e.g., [51]).

The Coastal Hazard Index (CHI) is aimed at including in the analysis the hazard assessment. It can be related to the probability that coastal flooding could actually threaten the coastal stretch. The CHI is defined as follows:

$$CHI = R_{50}, \tag{5}$$

where R_{50} is the return level of the 2% exceedance wave runup related to a return period equal to 50 years. The values of R_{50} may be estimated by means of a standard statistical inference (by considering the generalized extreme values’ probability distribution) on the wave runup induced by sea storms identified by Peak Over Threshold (POT) analysis (e.g., [53]). Table 2 synthesizes the ranking of the CHI defined with the same rationale employed to define the ranking of factors involved in the CVI definition.

Table 2. Ranking needed to evaluate the Coastal Hazard Index (CHI).

	Low (1)	Moderate (2)	High (3)	Very High (4)
CHI (m)	<1.0	1.0–1.5	1.5–2.0	>2.0

3. The Case Study of Montalto Di Castro

3.1. Site Description

Montalto di Castro's coastal stretch is located in the central Tyrrhenian Sea (northern part of Lazio Province, Italy) and oriented in a SE-NW direction (Figure 2). Sandy-muddy sediments, with an increase in the muddy fraction moving southwards and offshore [54], characterize the coastal zone. Relevant economic and commercial activities and typical Mediterranean environmental ecosystems are present in the area. The emerged beach is limited by coastal dune formation often established by coastal vegetation [55]. Coastal dunes are subject to periodic erosive processes in the northern part (between Ansedonia and the Arrone River), while they tend to increase in amplitude moving towards the south direction (between Montalto and Riva dei Tarquini), where dunes' width reaches the mean and highest values of about 100 m and 400 m, respectively [55]. The submerged beach is slightly sloping and presents an irregular sea bottom with several features (such as palaeoridges covered by recent sediments, palaeochannels and *Posidonia oceanica* meadows).

An in-depth analysis of the field data was performed in order to characterize typical water level and wave conditions. Based on the analysis of the water level collected by means of the mareographic station deployed in Civitavecchia Harbor, about 30 km to the southeast of the considered site (geographical location 42°05'38.25" N, 11°47'22.73" E, time interval spanning from 1986 up to 2015), the Highest Astronomical Tide (HAT) and the Lowest Astronomical Tide (LAT) measured with respect the mean water level are equal to about 20.0 cm and −18.0 cm, respectively, while the Mean High Water Spring (MHWS) and Mean Low Water Spring (MLWS) are equal to about 16.0 cm and −15.0 cm, and Mean Low Water Neap (MLWN) are equal to about 11.0 cm and −9.0 cm, respectively. The characterization of the meteorological tide (i.e., storm surge) led to an estimation of about 45 cm for frequent conditions (return period equal to two years) and about 65 cm for rare conditions (return period equal to 200 years). As far as wave climate is concerned, based on the analysis of the data provided by the ERA-interim research project (e.g., [36], computational point 42.0° N, 11.25° E), the considered site is characterized by an offshore mean significant wave height equal to about 0.90 m. The waves come mainly from the west, southwest and south sectors.

3.2. Data

The bathymetry used in the model scenario based on national scale data was obtained by triangular interpolation with respect to EMODnet point data [34] and the model grid. A 500-m resolution grid was first used, in order to produce proper boundary conditions for five nested grids with a resolution of 250 m (Figure 2). In particular, results corresponding to 5-m, 10-m and 20-m water depths were selected among all the cells in the nested grids. In this way, for each output point, a transfer function was defined as a table that contains H_{m0} and D_m corresponding to the coastal propagation of each selected offshore condition (see Section 2.1).

One of the nested grids was also used to perform the detailed model scenario. A high resolution topo-bathymetric dataset, for the selected case study, was obtained by merging topographic and bathymetric LiDAR data (acquired within the LIDLAZproject, on 9 May 2009 during good weather conditions [55]) and multibeam data (acquired from Lazio Province). LiDAR and multibeam data were processed to obtain the topographic and bathymetric configuration on regular grids (25 × 25 m).

Then, bathymetric data, obtained through triangular interpolation of the two merged layers, were used in the detailed modeling scenario.

The offshore wave climate has been evaluated using half hourly measurements collected by the directional wave buoy of Civitavecchia, about 50 km south from the Montalto di Castro coast (40°52'0.1" N, 12°56'60.0" E), belonging to the Italian Buoys Network. The analyzed wave data cover a 16-year period, from 1989–2005, and consist of significant wave height (H_{m0}), peak wave period (T_p) and mean wave direction (D_m). Furthermore, the wave data provided by the ERA-Interim research project were used in order to consider a wider temporal interval (spanning from 1979 up to 2015) of the wave observation.

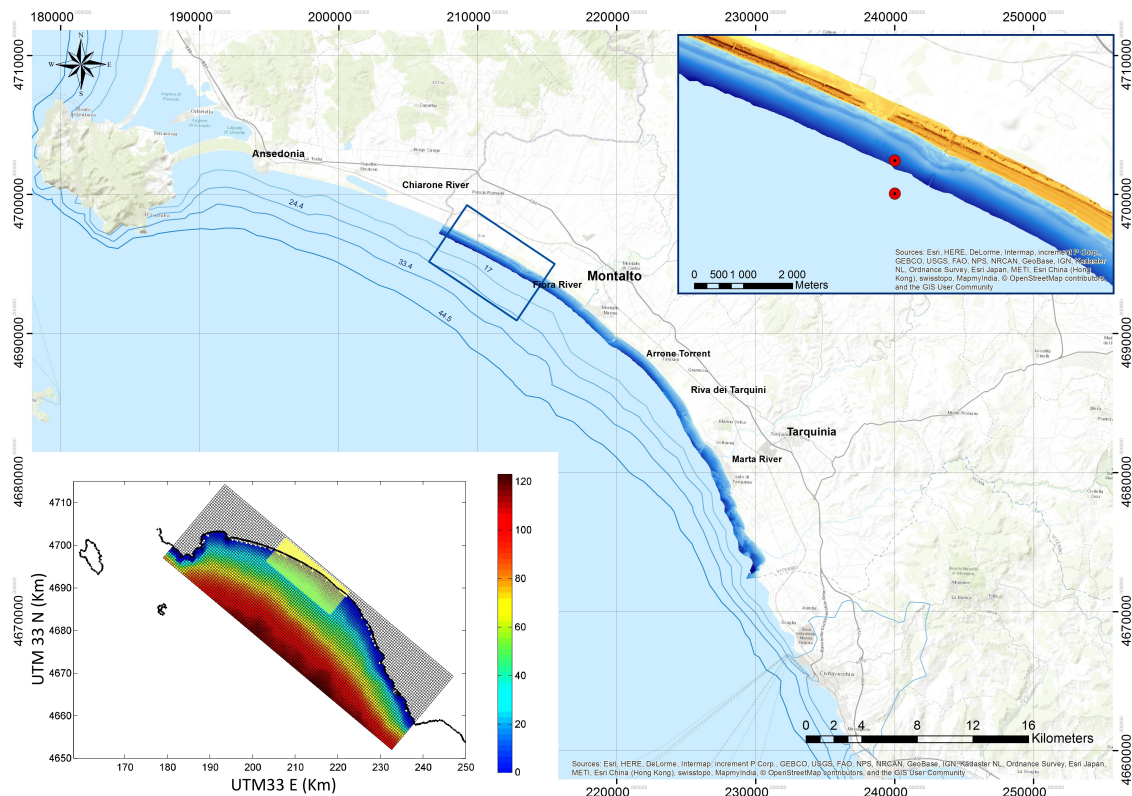


Figure 2. Montalto di Castro study area (Central Italy, Tyrrhenian Sea). The box in the bottom left report the grid of the numerical simulation (the color scale refers to the bathymetry based on EMODnet data). Both the large grid (500-m resolution) and the nested grid (250-m resolution) used for the comparison of two modeling scenarios are depicted. The box in the top right shows topo-bathymetric data used in the detailed model scenario (i.e., LiDAR data collected within the LIDLAZ project, Lidar Survey of the Lazio Province coastline, and multibeam data provided by Lazio Province). Red solid circles indicate to the points where the wave climate has been compared (the one closer to the coast refers to the detailed model scenario).

4. Results and Discussion

As already underlined, the analysis described herein is devoted to assessing the reliability of the results when national-scale data are used. Hence, the results obtained by using data known at the national scale are compared to those obtained when local-scale data (and rarely available at the national scale) are considered. Therefore, (a) nearshore wave parameters (i.e., significant wave height) and (b) empirical estimated wave runup obtained for the two scenarios have been compared. Then, the Coastal Vulnerability Index (CVI) and the Coastal Hazard Index (CHI) described in Section 2.3 have been estimated.

4.1. Nearshore Wave Parameters

As an example, the significant wave heights computed at the water depth of 10 m in approximately the middle position of the examined area were compared for the national- versus local-scale analyses (solid circles in Figure 2). Similar results are obtained for different locations along the coastal stretch.

The mean absolute difference between the significant wave height values of the two nearshore wave time series on the whole period is equal to 2.33 cm, while the mean difference (the differences being positive if the significant wave height is estimated by using national-scale data (H_{s-ns}) is higher than the ones obtained by using local scale data (H_{s-ls}) is equal to -1.74 cm. It could be useful to know that the mean value of the nearshore significant wave height evaluated on the basis of local scale data is equal to about 0.46 m. It has to be noticed that the mean nearshore significant wave height is lower than the mean offshore significant wave height as some of the offshore sea states cannot propagate toward the considered coastal stretch. Therefore, the use of national-scale data leads to a slight underestimation of significant wave height. This is confirmed by the kurtosis (greater than zero) and skewness (lower than zero) of the Empirical Probability Density Function (EPDF) of the differences (lower left panel of Figure 3) and by the best fit line slope equal to 1.06 (upper left panel of Figure 3), i.e., the significant wave heights computed by using local-scale data are about 6% higher, on average, than those computed by using national-scale data.

The same big picture may be drawn looking at the percentiles of the maximum significant wave height of sea storms identified by using a threshold value equal to 2.3 m within the frame of the standard Peak Over Threshold technique (POT method, right panels of Figure 3). On average, the percentiles estimated by using national-scale data (H_{s-ns}^p) are about 11% lower than the ones estimated by using local-scale data (H_{s-ls}^p , upper right panel of Figure 3). The underestimation observed when national-scale data are used is confirmed by the mean error of the difference between the percentiles estimated by using national-scale and local-scale data equal to -3.34 cm and the kurtosis and skewness of their EPDF (lower right panel of Figure 3). It has to be stressed that the results described herein in terms of nearshore wave parameters, evaluated at the 10-m contour depth, can be extended to other sites for which the beach morphodynamics can be supposed to be unimportant for such a water depth (i.e., roughly if the depth of closure is lower than 10 m, e.g., [56,57]).

4.2. Wave Runup

The wave runup has been estimated by using Formulation (2) proposed by Stockdon et al. [31]. The application of Equation (2) needs the evaluation of the offshore wave conditions (i.e., H_0 and L_0) and of the beach slope. For both national-scale and local-scale data, the beach slope has been evaluated by considering the mean slope of the vertical region whose height is two-times the breaking depth, considered as a measure of the standard deviation of the continuous water level record (the use of the standard deviation is suggested by Stockdon et al. [31]). The breaking depth has been simply estimated by means of linear theory and the 0.78-criterion (i.e., the ratio of breaking wave height to water depth equal to 0.78, e.g., [58]); moreover, also the mean slope of the vertical region from a representative depth up to the elevation equal to the breaking depth (emerged). The representative depth was selected equal to 10 m, as the local-scale bathymetric data reach a depth of about 12 m. It has to be stressed that the same methodology was proposed by Mather et al. [47] with a reference depth equal to 15 m. Hence, four estimations of the 2% exceedance wave runup have been carried out for the whole offshore wave time series and for 25 selected sections of the study site (distance between sections equal to 500 m). Two of them refer to the national-scale data (i.e., $R_{2-ns-hb}$ and $R_{2-ns-hr}$, the former being related to the mean slope defined on the basis of breaking depth (h_b) and the latter to the mean slope defined on the basis of the representative depth (h_r) and breaking depth) and two of them to the local-scale data ($R_{2-ls-hb}$ and $R_{2-ls-hr}$). The estimation achieved with local-scale data and by considering the mean

slope over the vertical region defined on the basis of breaking depth (i.e., R_{2-l_s-hb}) has been taken as the reference value. Then, the ratio R^* of the estimated 2% exceedance wave runup (i.e., $R_{2-ns-hb}$, $R_{2-ns-hr}$ and R_{2-l_s-hr}) to the reference value (i.e., R_{2-l_s-hb}) has been computed for the whole offshore time series. Figure 4 (upper panel) shows the percentiles of the EPDF of ratio R^* .

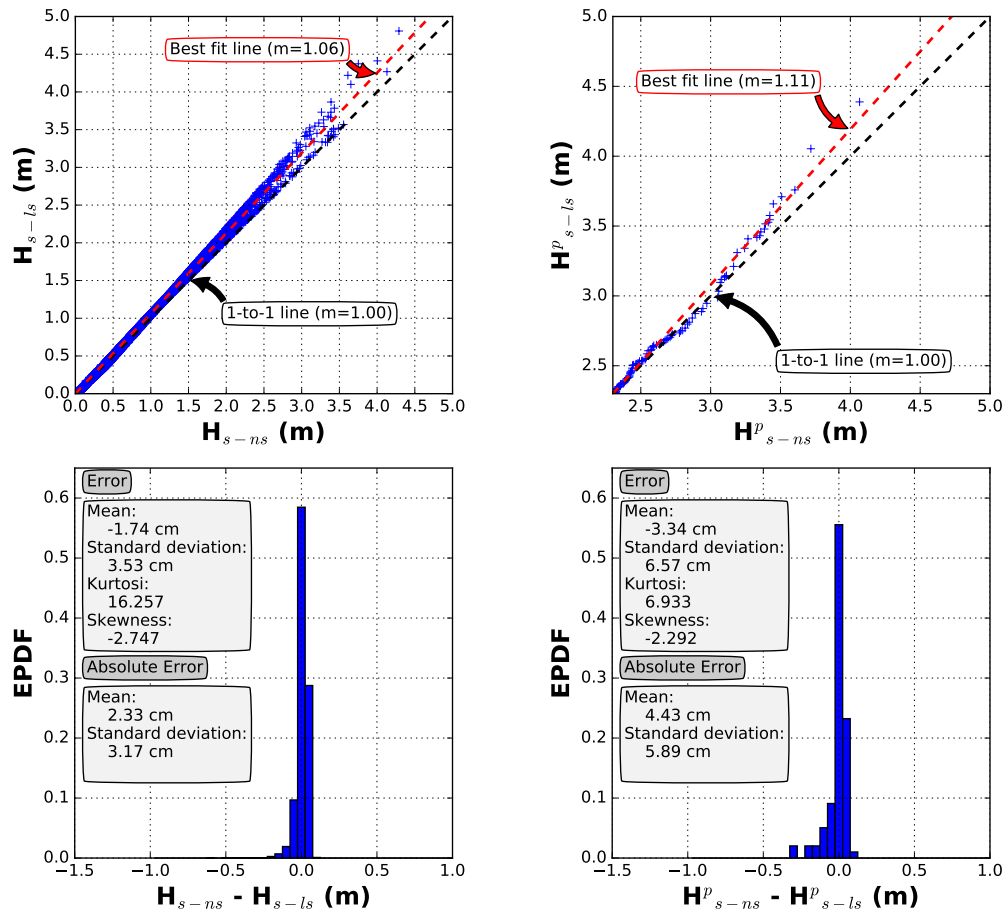


Figure 3. Nearshore wave parameters. (Left panels) Statistical analysis of the whole time series of nearshore significant wave height estimated by using national-scale data (H_{s-ns}) and local-scale data (H_{s-ls}); (right panels) statistical analysis of the percentiles of the maximum significant wave height of sea storms identified by a threshold equal to 2.3 m when national-scale data (H_{s-ns}^p) and local-scale data (H_{s-ls}^p) are used; (upper panels) scatter plots of significant wave height (either the whole time series or the maximum of each sea storm) estimated by using national-scale and local-scale data; (lower panels) Empirical Probability Density Function (EPDF) of the difference of the significant wave height (either the whole time series or the maximum of each sea storm) estimated by using national-scale and local-scale data (synthetic information is reported in each plot).

Moreover, the percentiles of EPDF of the maximum 2% exceedance wave runup of sea storms identified by the standard POT technique have been considered. Therefore, the ratio R^P of the percentiles of the EPDF of the estimated maximum 2% exceedance wave runup of sea storms (i.e., $R_{2-ns-hb}^P$, $R_{2-ns-hr}^P$ and $R_{2-l_s-hr}^P$) to the reference value (i.e., $R_{2-l_s-hb}^P$) has been computed. Figure 4A shows the percentiles of the EPDF of ratio R^P .

When the whole 2% exceedance wave runup time series is concerned (Figure 4A), the inspection of the results reveals that the use of national-scale data leads to the underestimation of the 2% exceedance wave runup. Nevertheless, the higher the percentile (i.e., the lower the exceedance probability), the lower the underestimation of 2% exceedance wave runup obtained by using national-scale data.

It should be noted that the use of reference depth to define the beach slope leads to the underestimation of the 2% exceedance wave runup with respect to the reference values, also if local-scale data are used (continuous line in Figure 4A). On the other hand, if the reference depth is used to define the beach slope by using national-scale data, the estimate of 2% exceedance wave runup is almost the same as the value estimated by using the beach slope evaluated on the basis of breaking depth. This could be expected, as it is almost trivial to observe that only detailed surveys may provide a reliable (and high spatial resolution) estimation of the beach slope close to the shore. From a quantitative point of view, the underestimation of the percentiles of the EPDF of the whole 2% exceedance wave runup time series is between 65% (low percentile ranks) and 25% (high percentile ranks), with a slight difference between $R_{2-ns-hr}^*$ and $R_{2-ns-hb}^*$.

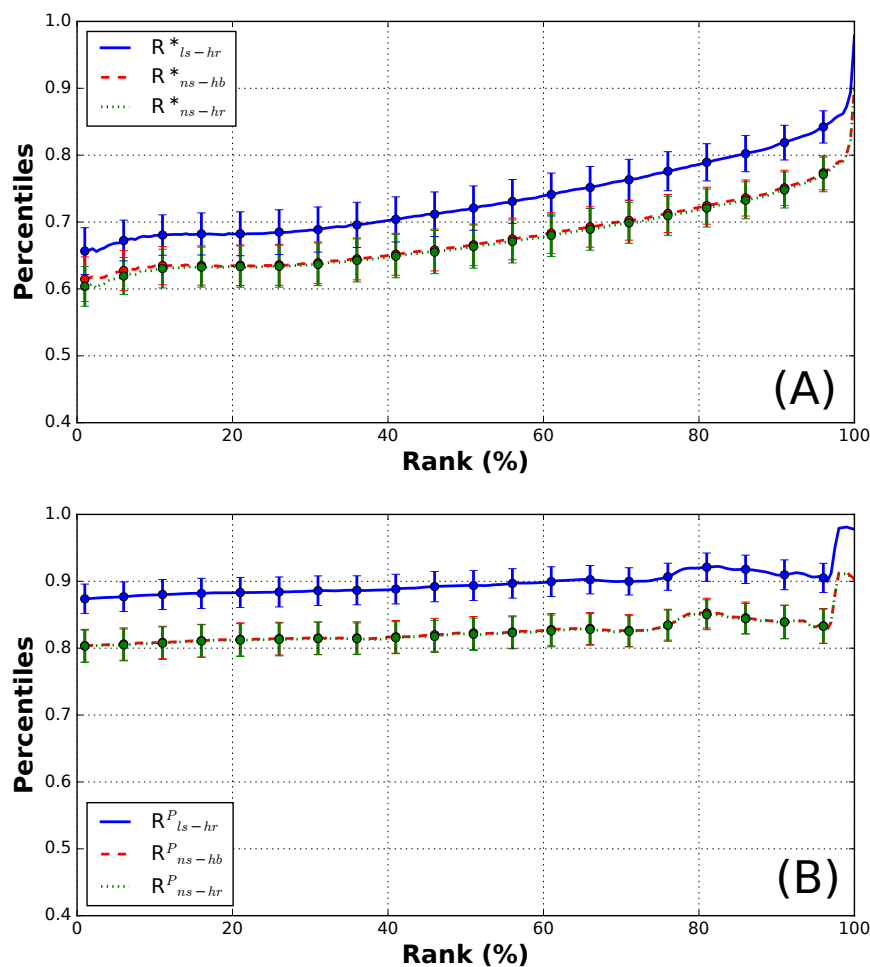


Figure 4. Wave runup. (A): percentiles of the EPDF of R^* (ratio of the percentiles of the EPDFs of the estimated whole 2% exceedance wave runup time series, i.e., $R_{2-ns-hb}^*$, $R_{2-ns-hr}^*$ and $R_{2-ls-hr}^*$, and the reference value, i.e., $R_{2-ls-hb}^*$); (B): percentiles of the EPDF of R^P (ratio of the percentiles of the EPDFs of the estimated maximum 2% exceedance wave runup of sea storms, i.e., $R_{2-ns-hb}^P$, $R_{2-ns-hr}^P$ and $R_{2-ls-hr}^P$, and the reference value, i.e., $R_{2-ls-hb}^P$). The error bars refer to the standard error.

When the maximum 2% exceedance wave runup of sea storms is concerned (Figure 4B), the underestimation observed when national-scale data are used decreases down to about 25% (percentiles higher than 0.8), almost constant with respect to the percentile ranks. In other words, the 2% exceedance wave runup estimation based on national-scale data becomes more reliable for extreme values. It has to be observed that high percentile ranks of the EPDF of maximum 2% exceedance wave

runup of sea storms are important for hazard assessment, as they are related to rather severe storms when coastal flooding is likely to occur.

It should be noted that the evaluation of the underestimation of wave runup is based on the assumption that the 2% exceedance wave runup estimated by using local-scale data is equal to the real one, at least very similar, i.e., that the formulation proposed by Stockdon et al. [31] is correct in reproducing the reality. Other runup formulations have been applied and some numerical simulations performed by using the swash numerical model (e.g., [59]), and almost the same big picture has been drawn on the basis of the results. However, it has to be strongly underlined that this paper focuses on the preliminary coastal flood risk assessment, when the reliability of empirical formulations usually suffices. Of course, when detailed studies are needed, specific numerical simulations have to be performed.

4.3. Coastal Vulnerability Index and Coastal Hazard Index

Each factor needed to compute the Coastal Vulnerability Index expressed by Equation (4) has been evaluated for a series of 25 cross-sections (distance between sections equal to 500 m) of the considered area. All the factors have been calculated twice: one time by using national-scale data, one time by using local-scale data. Figure 5 shows the values of the factors, for all 25 considered sections and for both national-scale and local-scale data, whilst Figure 6 shows the resulting CVI.

It can be observed that the differences are rather small for F_W (mean value of the annual maximum of significant wave height at the nearshore limit), whilst higher differences for factors F_S (slope of submerged beach), F_A (extension of the flooded area) and F_D (horizontal distance of the reference water depth) are observed. The small differences for F_W confirm the results in terms of nearshore wave parameters (see Section 4.1): the use of national-scale data does not significantly affect the reliability of the results. On the other hand, the use of national-scale data does not allow one to resolve the slope of the beach, neither in the submerged part nor in the emerged part.

In terms of CVI (Figure 6), the use of national-scale data tends to conservatively assess the vulnerability of the cross-sections along the considered coastal stretches. Indeed, the use of national-scale data tends to estimate a higher vulnerability than the use of local-scale data and, thus, is deemed more conservative. The term conservative is used hereinafter in order to indicate the safe (i.e., high) vulnerability or hazard assessments. For instance, if the analysis based on the use of national-scale data leads to higher vulnerability ranks than the ones evaluated on the basis of local-scale data, then the former analysis is conservative with respect to the latter. The main differences are related to the factor aimed at describing the extension of the area prone to be flooded. Then, Figure 7 shows the CVI evaluated on the basis of factors F_S (slope of submerged beach), F_D (horizontal distance of the reference water depth) and F_W (mean value of the annual maximum of significant wave height at the nearshore limit), then excluding the factor F_A (i.e., the extension of the flooded area). It can be observed that the discrepancies between the results achieved by using national-scale and local-scale data are less evident. The use of local-scale data leads to a moderate vulnerability assessment along the whole coastal stretch, while the use of national-scale data leads to assessing some proportion of the coastal stretch (about a half of the considered sections) as highly vulnerable.

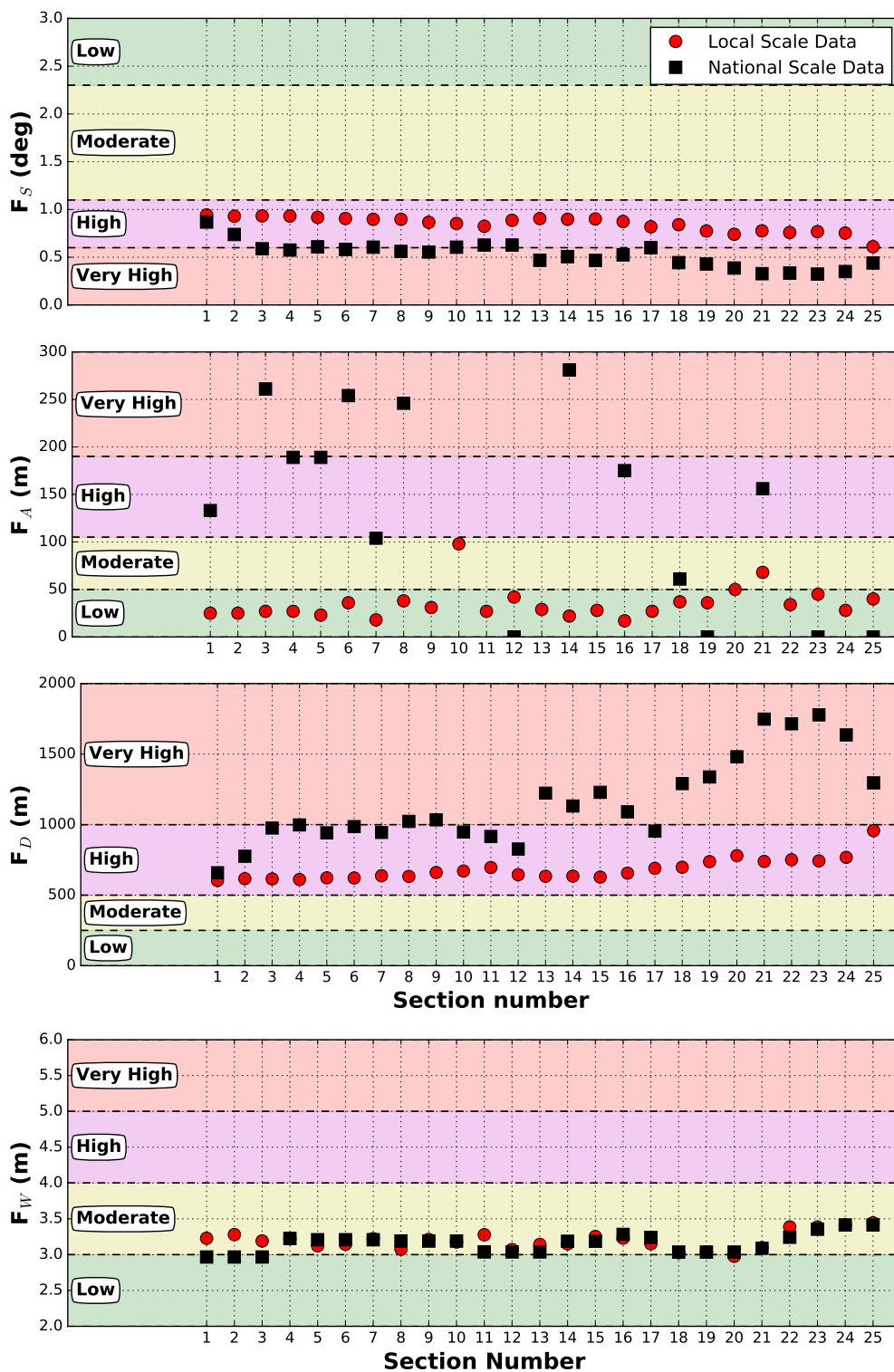


Figure 5. Factors for the Coastal Vulnerability Index (CVI) assessment. From the upper panel to the lower panel: F_S (slope of submerged beach), F_A (extension of the flooded area), F_D (horizontal distance of the reference water depth, i.e., 10 m, from the coastline), F_W (mean value of the annual maximum of significant wave height at the nearshore limit) evaluated for each cross-section (the x axis reports the section numbering; see Figures 6–8) along the considered coastal stretch. The shaded areas refer to the vulnerability levels.

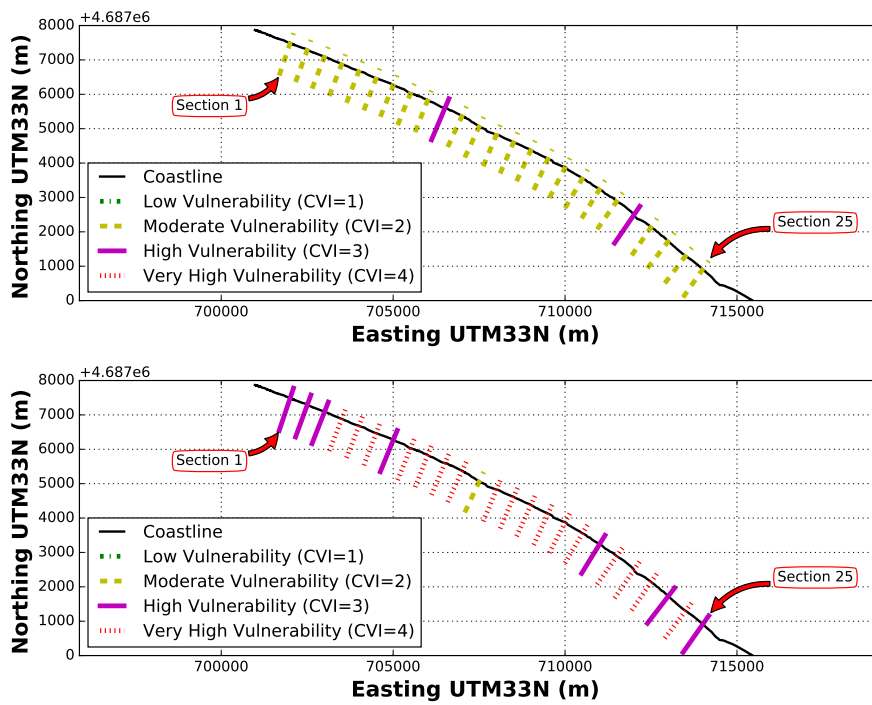


Figure 6. Coastal Vulnerability Index (CVI) for all the considered cross-sections by using local-scale data (upper panel) and national-scale data (lower panel). Section numbering, from 1–25, starts from north.

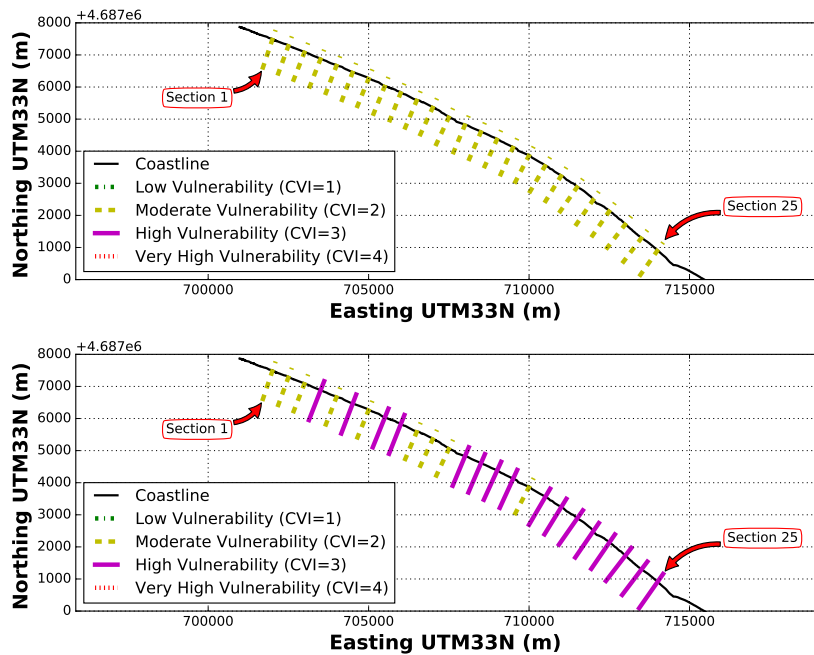


Figure 7. Coastal Vulnerability Index (CVI) for all the considered cross-sections by using local-scale data (upper panel) and national-scale data (lower panel) evaluated by excluding the factor F_A (i.e., extension of the flooded area). Section numbering, from 1–25, starts from north.

Furthermore, the CHI has been evaluated twice: one time by using national-scale data ($R_{2-ns-hr}$), one time by using local-scale data ($R_{2-ls-hb}$). Figure 8 shows the results in terms of CHI for each cross-section evaluated by using both national-scale and local-scale data. It can be observed that the use of national-scale data tends to unconservatively assess the coastal hazard. Of course, this is

expected in view of the discussion related to wave runup (see Section 4.2): as the wave runup is underestimated by using national-scale data, then the hazard is unconservatively assessed with respect to the results obtained by using local-scale data. The CHIs are much more similar between the local and national scale: the use of national-scale data leads to a lower CHI estimate on only three of 25 stretches. Nevertheless, if the 2% exceedance wave runup estimated on the basis of national-scale data and amplified by a factor equal to 1.25 (as found in Section 4.2) is used, the CHI assessment is conservative (Figure 8, lower panel).

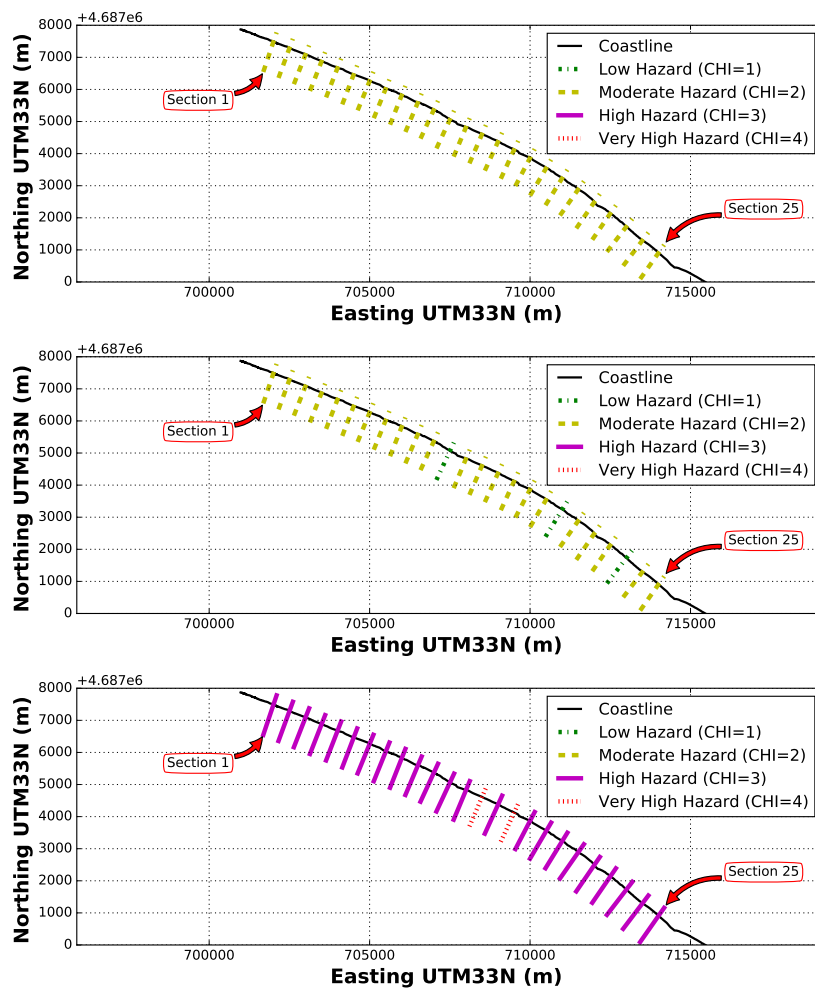


Figure 8. Coastal Hazard Index (CHI) for all the considered cross-sections by using local-scale data (upper panel) and national-scale data (middle panel). (Lower panel) The CHI evaluated by using national-scale data and by amplifying the estimated 2% exceedance wave runup by a factor equal to 1.25. Section numbering, from 1–25, starts from north.

5. Concluding Remarks and Ongoing Research

This paper aims to illustrate the first steps of a research project for assessing coastal vulnerability to wave-induced flooding at the national scale. One of the aims of the project is to perform a comparative analysis related to the availability of information at the national scale. The analysis was performed for the area of Montalto di Castro, a dissipative sandy beach (Tyrrhenian Sea, Italy), by using datasets with different spatial resolutions.

First, the results show that the estimated nearshore wave features are not significantly influenced by the differences of bathymetric data. If the wave runup is concerned, it was observed that it is

underestimated by using field data available at the national scale by about 25% if sea storms are considered. Indeed, it was shown that the method applied using low resolution datasets retains its reliability if extreme events are considered (i.e., high energy events). Then, the results obtained by using data available at the national scale may be of sufficient reliability for the development of criteria for the preliminary assessment of coastal vulnerability and hazard related to flooding, thus useful as a decision support tool for coastal zone management and to select the area where more detailed analysis is needed. Indeed, as also the Floods Directive 2007/60/EC suggests, a national-scale preliminary analysis should be performed in order to identify the coastal areas that deserve to be analyzed in more detail. Then, the detailed analysis (i.e., by using local-scale data) could be performed for a limited number of coastal areas. It has to be stressed that the results of the preliminary analysis (and fast if compared to a detailed study) are conservative. In other words, the results of the study presented herein show that, at least for dissipative beaches, as the coastal stretch considered herein, the use of data available at the national scale allows one to conservatively identify areas that should undergo detailed analysis.

The research project is still in progress with two main aims: first, to validate the fast method described in this paper (i.e., the preliminary analyses based on the use of field data available at the national scale) by using wave runup data measured by means of a video monitoring system; then, the reliability of the hazard assessment could be compared to real data instead of empirical formulations. The second aim of the ongoing research is to complete the method with the exposure evaluation (by using both local-scale and national-scale data) in order to evaluate the coastal flooding risk (i.e., not only vulnerability and hazard).

Acknowledgments: The authors would like to acknowledge Luisa Nicoletti and Andrea Taramelli for giving LiDAR data (acquired within the LIDLAZ project founded by the Lazio-Region Local Authority). Thanks to Eng. Paolo Lupino and Alessandro Bratti (Lazio Region-Local Authority) for giving Multibeam data. Thanks to Massimo Gabellini (ISPRA) for encouraging the research activities. The authors are also grateful to Emiliano Canali, Raffaele Proietti, Lorenzo Rossi and Andrea Salmieri (ISPRA) for providing useful help in handling bathymetric data.

Author Contributions: All the authors contributed equally to this work.

Conflicts of Interest: The authors declare no conflict of interest.

References

1. Meur-Férec, C.; Deboudt, P.; Morel, V. Coastal risks in France: An integrated method for evaluating vulnerability. *J. Coast. Res.* **2008**, *24*, 178–189.
2. Ciavola, P.; Armaroli, C.; Perini, L.; Luciani, P. Evaluation of maximum storm wave run-up and surges along the Emilia-Romagna coastline (NE Italy): A step towards a risk zonation in support of local CZM strategies. In *Integrated Coastal Zone Management-The Global Challenge*; Kannen, A., Ramanathan, A., Glavovic, B.C., Green, D.R., Krishnamurthy, R.R., Tinti, S., Agardy, T., Han, Z., Eds.; Research Publishing Services: Oxford, UK, 2008; Chapter 16, pp. 505–516.
3. De Girolamo, P.; Di Risio, M.; Romano, A.; Molfetta, M. Landslide Tsunami: Physical Modeling for the Implementation of Tsunami Early Warning Systems in the Mediterranean Sea. *Procedia Eng.* **2014**, *70*, 429–438, doi:10.1016/j.proeng.2014.02.048
4. Perini, L.; Calabrese, L.; Salerno, G.; Ciavola, P.; Armaroli, C. Evaluation of coastal vulnerability to flooding: Comparison of two different methodologies adopted by the Emilia-Romagna region (Italy). *Nat. Hazards Earth Syst. Sci.* **2016**, *16*, 181–194.
5. Spaulding, M.L.; Grilli, A.; Damon, C.; Crean, T.; Fugate, G.; Oakley, B.A.; Stempel, P. STORMTOOLS: coastal environmental risk index (CERI). *J. Mar. Sci. Eng.* **2016**, *4*, 54.
6. Nageswara Rao, K.; Subraelu, P.; Venkateswara Rao, T.; Hema Malini, B.; Ratheesh, R.; Bhattacharya, S.; Rajawat, A.S.; Ajai. Sea-level rise and coastal vulnerability: An assessment of Andhra Pradesh coast, India through remote sensing and GIS. *J. Coast. Conserv.* **2008**, *12*, 195–207.

7. Di Risio, M.; Lisi, I.; Beltrami, G.; De Girolamo, P. Physical modeling of the cross-shore short-term evolution of protected and unprotected beach nourishments. *Ocean Eng.* **2010**, *37*, 777–789, doi:10.1016/j.oceaneng.2010.02.008
8. Mendoza, E.T.; Ojeda, E.; Meyer-Arendt, K.J.; Salles, P.; Appendini, C.M. Assessing Coastal Vulnerability in Yucatan (Mexico). *Coast. Manag.* **2016**, 607–616, doi:10.1680/cm.61149.607.
9. Tapsell, S.; McCarthy, S.; Faulkner, H.; Alexander, M. *Social Vulnerability to Natural Hazards*; CapHaz-Net WP4 Report; Flood Hazard Research Centre—FHRC, Middlesex University: London, UK, 2010.
10. Silva, S.F.; Martinho, M.; Capitão, R.; Reis, T.; Fortes, C.J.; Ferreira, J.C. An index-based method for coastal-flood risk assessment in low-lying areas (Costa de Caparica, Portugal). *Ocean Coast. Manag.* **2017**, *144*, 90–104.
11. De Bruijn, K.; Klijn, F.; Ölfert, A.; Penning-Rowsell, E.; Simm, J.; Wallis, M. *Flood Risk Assessment and Flood Risk Management; An Introduction and Guidance Based on Experiences and Findings of FLOODsite (An EU-Funded Integrated Project)*; T29-09-01; FLOODsite Consortium: Wallingford, UK, 2009.
12. Gornitz, V.M.; Daniels, R.C.; White, T.W.; Birdwell, K.R. The development of a coastal risk assessment database: vulnerability to sea-level rise in the US Southeast. *J. Coast. Res.* **1994**, pp. 327–338.
13. De Moel, H.; van Alphen, J.; Aerts, J.C.J.H. Flood maps in Europe: Methods, availability and use. *Nat. Hazards Earth Syst. Sci.* **2009**, *9*, 289–301.
14. Archetti, R.; Paci, A.; Carniel, S.; Bonaldo, D. Optimal index related to the shoreline dynamics during a storm: The case of Jesolo beach. *Nat. Hazards Earth Syst. Sci.* **2016**, *16*, 1107–1122.
15. La Valle, P.; Paganelli, D.; Ercole, S.; Lisi, I.; Teofili, C.; Nicoletti, L. Coastal Management and Environmental Guidelines Related to Coastal Defence Works. In *Changing Coast, Changing Climate, Changing Minds*; ICE Publishing: London, UK, 2016; pp. 69–75.
16. Torresan, S.; Critto, A.; Dalla Valle, M.; Harvey, N.; Marcomini, A. Assessing coastal vulnerability to climate change: Comparing segmentation at global and regional scales. *Sustain. Sci.* **2008**, *3*, 45–65.
17. Hinkel, J.; Klein, R.J. Integrating knowledge to assess coastal vulnerability to sea-level rise: The development of the DIVA tool. *Glob. Environ. Chang.* **2009**, *19*, 384–395.
18. Ciavola, P.; Ferreira, O.; Dongeren, A.V.; Vries, J.V.T.D.; Armaroli, C.; Harley, M. Prediction of Storm Impacts on Beach and Dune Systems. In *Hydrometeorological Hazards: Interfacing Science and Policy*, 1st ed.; Philippe, Q., Ed.; John Wiley & Sons, Ltd.: Hoboken, NJ, USA, 2015; pp. 227–252.
19. Narra, P.; Coelho, C.; Sancho, F.; Palalane, J. CERA: An open-source tool for coastal erosion risk assessment. *Ocean Coast. Manag.* **2017**, *142*, 1–14.
20. Melby, J.A. *Wave Runup Prediction for Flood Hazard Assessment*; US Army Engineer Research and Development Center, Coastal and Hydraulics Laboratory: Vicksburg, MS, USA, 2012.
21. Roux, A.P. A Re-Assessment of Wave Run Up Formulae. Ph.D. Thesis, Stellenbosch University, Stellenbosch, South Africa, 2015.
22. Douglass, S.L. Estimating extreme values of run-up on beaches. *J. Waterw. Port Coast. Ocean Eng.* **1992**, *118*, 220–224.
23. Granthem, K.N. Wave Run-up on sloping structures. *Eos Trans. Am. Geophys. Union* **1953**, *34*, 720–724.
24. Saville, T., Jr. Wave Run-Up on Composite Slopes. *Coast. Eng. Proc.* **1957**, *1*, 41.
25. Savage, R.P. Wave run-up on roughened and permeable slopes. *Trans. Am. Soc. Civ. Eng.* **1959**, *124*, 852–870.
26. Hunt, I.A. Design of sea-walls and breakwaters. *Trans. Am. Soc. Civ. Eng.* **1959**, *126*, 542–570.
27. Wassing, F. Model investigation on wave run-up carried out in the Netherlands during the past twenty years. *Coast. Eng. Proc.* **1957**, *1*, 42.
28. Battjes, J.A. *Computation of Set-Up, Longshore Currents, Run-Up and Overtopping Due to Wind-Generated Waves*; Department of Civil Engineering, Delft University of Technology: Delft, The Netherlands, 1974.
29. Holman, R. Extreme value statistics for wave run-up on a natural beach. *Coast. Eng.* **1986**, *9*, 527–544.
30. Nielsen, P.; Hanslow, D.J. Wave runup distributions on natural beaches. *J. Coast. Res.* **1991**, *7*, 1139–1152.
31. Stockdon, H.F.; Holman, R.A.; Howd, P.A.; Sallenger, A.H. Empirical parameterization of setup, swash, and runup. *Coast. Eng.* **2006**, *53*, 573–588.
32. De la Peña, J.; Sanchez, J.; Diaz, R.; Martin, M. Physical model and revision of theoretical runup. *Coast. Eng. Proc.* **2012**, *1*, 22.

33. Robinson, N.; Regetz, J.; Guralnick, R.P. EarthEnv-DEM90: A nearly-global, void-free, multi-scale smoothed, 90 m digital elevation model from fused ASTER and SRTM data. *ISPRS J. Photogramm. Remote Sens.* **2014**, *87*, 57–67.
34. Schaap, D.; Schmitt, T. EMODnet High Resolution Seabed Mapping—further developing a high resolution digital bathymetry for European seas. In Proceedings of the EGU General Assembly Conference Abstracts, Vienna, Austria, 23–28 April 2017; Volume 19, p. 4371.
35. Bencivenga, M.; Nardone, G.; Ruggiero, F.; Calore, D. The Italian data buoy network (RON). *Adv. Fluid Mech. IX* **2012**, *74*, 321.
36. Dee, D.; Uppala, S.; Simmons, A.; Berrisford, P.; Poli, P.; Kobayashi, S.; Andrae, U.; Balmaseda, M.; Balsamo, G.; Bauer, P.; et al. The ERA-Interim reanalysis: Configuration and performance of the data assimilation system. *Q. J. R. Meteorol. Soc.* **2011**, *137*, 553–597.
37. Booij, N.; Ris, R.; Holthuijsen, L.H. A third-generation wave model for coastal regions: 1. Model description and validation. *J. Geophys. Res. Oceans* **1999**, *104*, 7649–7666.
38. De Girolamo, P.; Di Risio, M.; Beltrami, G.; Bellotti, G.; Pasquali, D. The use of wave forecasts for maritime activities safety assessment. *Appl. Ocean Res.* **2017**, *62*, 18–26, doi:10.1016/j.apor.2016.11.006
39. Van der Meer, J.; Allsop, N.; Bruce, T.; De Rouck, J.; Kortenhaus, A.; Pullen, T.; Schtrumpf, H.; Troch, P.; Zanuttigh, B. *EurOtop: Manual on Wave Overtopping of Sea Defences and Related Structures—An Overtopping Manual Largely Based on European Research, but for Worldwide Application*; Van der Meer Consulting: Akkrum, The Netherlands, 2016.
40. Guza, R.T.; Thornton, E.B. Swash oscillations on a natural beach. *J. Geophys. Res. Oceans* **1982**, *87*, 483–491.
41. Holman, R.A.; Sallenger, A.H. Setup and swash on a natural beach. *J. Geophys. Res. Oceans* **1985**, *90*, 945–953.
42. Iwagaki, H.M.Y. Run-Up of Random Waves on Gentle Slopes. In Proceedings of the 19th International Conference on Coastal Engineering, Houston, TX, USA, 3–7 September 1984.
43. Mase, H. Random Wave Runup Height on Gentle Slope. *J. Waterw. Port Coast. Ocean Eng.* **1989**, *115*, 649–661.
44. Ruggiero, P.; Komar, P.D.; McDougal, W.G.; Marra, J.J.; Beach, R.A. Wave runup, extreme water levels and the erosion of properties backing beaches. *J. Coast. Res.* **2001**, *17*, 407–419. doi:10.1061/9780872624382.041.
45. Park, H.; Cox, D.T. Empirical wave run-up formula for wave, storm surge and berm width. *Coast. Eng.* **2016**, *115*, 67–78.
46. Roberts, T.M.; Wang, P.; Kraus, N.C. Limits of wave runup and corresponding beach-profile change from large-scale laboratory data. *J. Coast. Res.* **2010**, *26*, 184–198.
47. Mather, A.; Stretch, D.; Garland, G. Predicting extreme wave run-up on natural beaches for coastal planning and management. *Coast. Eng. J.* **2011**, *53*, 87–109.
48. Polidoro, A.; Dornbusch, U.; Pullen, T. Improved maximum run-up formula for mixed beaches based on field data. *From Sea to Shore—Meeting the Challenges of the Sea: (Coasts, Marine Structures and Breakwaters 2013, Edinburgh, UK)*; ICE Publishing: London, UK, 2014; pp. 389–398.
49. Thieler, E.; Hammar-Klose, E. *National Assessment of Coastal Vulnerability to Future Sea Level Rise: Preliminary Results for the U.S. Atlantic Coast*; Technical Report Open-File Report 99-593; U.S. Geological Survey: Reston, VA, USA, 1999.
50. Yin, J.; Yin, Z.; Wang, J.; Xu, S. National assessment of coastal vulnerability to sea-level rise for the Chinese coast. *J. Coast. Conserv.* **2012**, *16*, 123–133.
51. Martínez-Graña, A.; Boski, T.; Goy, J.; Zazo, C.; Dabrio, C. Coastal-flood risk management in central Algarve: Vulnerability and flood risk indices (South Portugal). *Ecol. Indic.* **2016**, *71*, 302–316.
52. Pasquali, D.; Di Risio, M.; De Girolamo, P. A simplified real time method to forecast semi-enclosed basins storm surge. *Estuar. Coast. Shelf Sci.* **2015**, *165*, 61–69, doi:10.1016/j.ecss.2015.09.002
53. Goda, Y. *Random Seas and Design of Maritime Structures*; World Scientific: Singapore, 2010.
54. Paganelli, D.; Nonnis, O.; Finioia, M.G.; Gabellini, M. The role of sediment characterization in environmental studies to assess the effect of relict sand dredging for beach nourishment: The example of offshore sand deposits in Lazio (Tyrrhenian Sea). *J. Coast. Res.* **2013**, *65*, 1015–1020.
55. ISPRA. *Rilievo di Dettaglio Della Batimetria Costiera Laziale Con Tecnologie Lidar e Valutazione Delle Caratteristiche Fisiche e Biologiche in Aree Marine Della Costa Laziale di Specifico Interesse Ambientale*; Technical Report; ISPRA: Rome, Italy, 2009. (In Italian)
56. Nicholls, R.J.; Birkemeier, W.A.; Lee, G.H. Evaluation of depth of closure using data from Duck, NC, USA. *Mar. Geol.* **1998**, *148*, 179–201.

57. Lisi, I.; Bruschi, A.; Del Gizzo, M.; Archina, M.; Barbano, A.; Corsini, S. *Physiographic Units and Depths of Closure for the Italian Coast*; L'Acqua, Associazione Idrotecnica Italiana: Rome, Italy, 2010; pp. 35–52. (In Italian)
58. Dally, W.R.; Dean, R.G.; Dalrymple, R.A. Wave height variation across beaches of arbitrary profile. *J. Geophys. Res. Oceans* **1985**, *90*, 11917–11927.
59. Zijlema, M.; Stelling, G.; Smit, P. SWASH: An operational public domain code for simulating wave fields and rapidly varied flows in coastal waters. *Coast. Eng.* **2011**, *58*, 992–1012.



© 2017 by the authors. Licensee MDPI, Basel, Switzerland. This article is an open access article distributed under the terms and conditions of the Creative Commons Attribution (CC BY) license (<http://creativecommons.org/licenses/by/4.0/>).